Oxygenation of the Archean atmosphere: New paleosol constraints from Eastern India

Joydip Mukhopadhyay[1,3], Quentin G. Crowley[2#], Sampa Ghosh[1], Gautam Ghosh[1], Kalyan Chakrabarti[1,4], B. Misra[1,4], Kyle Heron[2] and Sankar Bose[1]

[1]Department of Geology, Presidency University, Kolkata, India,

[2] Department of Geology, School of Natural Sciences, Trinity College Dublin, Ireland

[3] PPM Research Group, Department of Geology, University of Johannesburg, Johannesburg

[4]Atomic Minerals Directorate, Eastern Region, Jamshedpur, India

#Communicating author: E-mail: crowleyq@tcd.ie

ABSTRACT

It is widely believed that atmospheric oxygen saturation rose from <10^{-5} Present Atmospheric Level (PAL) in the Archean to >10^{-2} PAL at the Great Oxidation Event (GOE) around 2.4 billion years ago, but it is unclear if any earlier oxygenation events occurred. Here we report U-Pb zircon data indicating a pyrophyllite-bearing paleosol, from Keonjhar in the Precambrian Singhbhum Craton of eastern India, formed between 3.29 and 3.02 billion years ago, making it one of very few known Archean paleosols globally. Field and geochemical evidence suggests that the upper part of the paleosol was eroded prior to unconformable deposition of an overlying sequence of shallow-marine siliciclastic sediments. A negative cerium anomaly within the currently preserved level of the paleosol indicates that ancient oxidative weathering occurred in the original upper soil profile. The presence of redox sensitive detrital uraninite and pyrite together with a complete absence of pyrophyllite in the overlying sediments indicate that the mineralogical and geochemical features of the paleosol were

established prior to unconformable deposition of the sediments and are not related to subsequent diagenetic or hydrothermal effects. We suggest a transient atmospheric oxygenation event occurred at least 600 million years prior to the GOE and approximately 60 million years prior to a previously documented Archean oxygenation event. We propose that several pulsed and short-lived oxygenation events are likely to have occurred prior to the GOE and that these changes to atmospheric composition arose due to the presence of organisms capable of oxygenic photosynthesis.

Key Words: Paleosol; atmospheric oxygen; Archean; detrital zircon; Singhbhum Craton

INTRODUCTION

Paleosols are ancient soil horizons formed by terrestrial weathering of rock surfaces. They preserve chemical records of atmospheric composition and various biotic or abiotic mediated chemical weathering pathways at the time of their formation. Paleosols from "deep time" provide a valuable opportunity to study evolution of the early atmosphere and emergence of distinct processes on Earth (Bekker et al., 2004; Holland, 2006). Very few Archean paleosols have been documented worldwide; these include the Pilbara (Johnson et al., 2008; 3.4 billion years (Ga) old), Nsuze (Crowe et al., 2013; c. 2.96 Ga) and Mt Roe (Macfarlane et al., 1994; 2.76 Ga) paleosols. The Pilbara and Mt. Roe paleosols, both of which occur in Pilbara NW Australia, indicate surface weathering took place in an oxygen poor atmosphere (Macfarlane et al., 1994; Yang et al., 2002), although controversy exists surrounding the Mt Roe Paleosols in that some studies suggest oxygen was present (Ohmoto, 1996; Phillippot et al., 2013). Recent work on the Nsuze Paleosol (Crowe et al., 2013) from the Pongola Supergroup of South Africa suggests that by 2.96 Ga oxygen levels had risen to at least 3×10^{-4} PAL, thus extending the chemical record of the first appreciable levels of atmospheric oxygen by about 500 million years.

Here we describe a previously undated supra-crustal sequence in the Singhbhum Craton of eastern India. We demonstrate that a paleosol, termed the Keonjhar Paleosol, formed between 3.29 and 3.02 Ga and did so in the presence of molecular oxygen. This is the world's oldest documented example of oxidative weathering. These findings further push back the age at which a pre-GOE oxygenation of the Earth's atmosphere occurred. By integrating our findings with those from Archean supra-crustal rocks, we give additional support to proposed models for both a pre-GOE oxygenation (Anbar, 2007; Crowe et al., 2013; Planavsky et al., 2014) and fluctuating Archean atmospheric oxygen levels (Lyons et al., 2014; Rosing & Frei, 2004).

GEOLOGICAL SETTING

The Keonjhar Paleosol has previously been described; however there have been no radiometric age constraints on its formation and it was speculated to be Palaeoproterozoic in age (Bandopadhyay et al., 2010). The paleosol occurs between a Paleo- to Mesoarchean (3.3 to 3.1 Ga) multi-component tonalite-trondhjemite-grandiorite (TTG) batholith known as the Singhbhum Granite and a thick unconformable succession of shallow-marine quartzarenite sandstones and interbedded conglomerates (Fig. 1A). These siliciclastic sediments are exposed along a near continuous outcrop bordering a Paleoarchean (3.51 to 3.3 Ga) greenstone belt termed the Iron Ore Group (Mukhopadhyay et al., 2008; Mukhopadhyay et al., 2012). The quartzarenite sandstones are known as the Mahagiri Quartzite in the southeast and the Pal Lahara-Mankaharchua Quartzite in the west, along a southeast-northwest transect of over 100 km from the town of Keonjhar (Fig. 1A). One part of the sandstone outcrop also extends north for over 80 km from Keonjhar. A clear angular unconformity exists between the sandstones and underlying greenstone belt rocks as well as the TTG granitoids (Mukhopadhyay et al., 2012). The best exposures of Keonjhar Paleosol occur around Madrangijori village, 6 km north of Keonjhar (Fig. 1A). Here quartzarenite sandstones can be observed unconformably overlying the paleosol (Fig. 1B), which passes downwards into altered granite. The paleosol thickness varies from one metre to more than six metres and is distinguished by its contrasting pale colour and talc-like feel. Petrographically the paleosol is dominantly composed of pyrophyllite and quartz (Fig. 1C), with subordinate amounts of illite and muscovite. Pyrophyllite formed from kaolinite and quartz in very low grade metamorphic conditions, whereas kaolinite formed due to chemical weathering of feldspar from the original granite. Pyrophyllite does not occur in the overlying sediments; therefore the chemical weathering which originally resulted in formation of the paleosol predates deposition of the unconformably overlying sediments. The siliciclastics from this region contain detrital uraninite and pyrite (Fig. 1D, E), which have also previously been described from quartz pebble conglomerates near the western margin of the Bonai Granite (Fig. 1) (Kumar et al., 2012). The presence of detrital uraninite and pyrite is significant in that they illustrate surface oxygen conditions did not exceed 10^{-3} PAL (Canfield et al., 2000) at the time of their deposition.

AGE OF THE KEONJHAR PALEOSOL

A component of the Singhbhum Granite, termed the Keonjhara-Bhaunra Granite, forms the "basement" to the paleosol. It has been dated at c. 3.29 Ga (Tait et al., 2011) and represents the oldest possible age of formation of the Keonjhar Paleosol. Here we present U-Pb detrital zircon age spectra from seven representative samples (Table DR1) of the entire quartzarenite sandstone outcrop belt. Our samples cover an extensive geographic area (Fig. 1), so constitute representative detrital zircon populations to limit the sedimentation age of the sandstones and provide an upper age bracket for the formation of the Keonjhar Paleosol. U-Pb detrital zircon ages from seven samples and 431 out of 770 analyses which are less than 10% discordant reveal detrital zircons between c. 3.58 and 3.02 Ga (Fig. 2A). The youngest detrital zircon population (3.02 Ga) was derived from a source significantly younger than the underlying granite. Overall, detrital zircon data indicate sandstones formed by recycling of several sources of pre-existing zircon-bearing differentiated crust. It is not possible to accurately estimate the time span between formation of the Keonjhar Paleosol and a change in relative sea level which resulted in unconformable deposition of the overlying siliciclastic sediments. The Keonjhar Paleosol is therefore conservatively constrained as having formed between crystallisation of the Keonjhara-Bhaunra Granite and the youngest detrital zircon population in the overlying sandstones; between 3.29 and 3.02 Ga. Consideration is also given to the possibility that the sediments may be considerably younger than suggested by the youngest detrital zircons. The presence of redox-sensitive detrital pyrite and uraninite in these sediments signifies pre-GOE deposition which could potentially be compatible with an earliest Paleoproterozoic age. Other stratigraphic units now preserved in different parts of the Singhbhum Craton (e.g. Dhanjori, Singhbhum and Kolhan Groups) contain abundant detrital zircons ranging from Neoarchean to Paleoproterozoic or Mesoproterozoic in age (Acharyya et al., 2010 and our unpublished U-Pb detrital zircon data from the Kolhan Group). In this respect, the absence of Proterozoic detrital zircons from the siliciclastic sediments immediately overlying the Keonjhar Paleosol is a direct consequence of their Archean depositional age and is not an artefact of the restricted availability of younger zircons in the supracrustals of this region. Additionally, we have observed 2.8 Ga granitoids (Misra et al., 2000) intruding Mahagiri Range quartzarenites (DT area in Fig. 1A), thus giving a minimum 2.8 Ga age to this entire Archean supra-crustal succession. This unequivocally places the Keonjhar Paleosol as amongst the oldest known such example on Earth, having formed sometime between the Pilbara and Nusze paleosols.

GEOCHEMISTRY OF THE PALEOSOL

Major, trace and Rare Earth Element (REE) compositions Keonjhar Paleosol samples devoid of surficial weathering have been determined (Table DR2). In order to characterize the alteration profile molar ratios of (i) immobile, (ii) redox sensitive and (iii) mobile elements are plotted relative to Ti (Fig. 2B), as the latter is considered relatively immobile during weathering. Exposures of unaltered “basement” granite were not observed in paleosol sample locations, so for comparative purposes nearby fresh Keonjhar-Bhaunra Granite (Fig. 1) compositions (Tait et al., 2011) have been selected to assess chemical alteration with respect to representative paleosol protolith compositions. Paleosol immobile element ratios (e.g. Al/Ti, Nb/Ti, Ga/Ti and Y/Ti) are generally within ranges shown by the granite, indicating the paleosol is *in situ*. A decrease in Th/Ti paleosol values suggests mobility of Th and likely involvement of acidic fluids during pedogenesis (Langmuir, 1997). Redox sensitive element ratios such as Fe_T/Ti and Mn/Ti are lower in the paleosol profile, whereas V/Ti is generally higher relative to the granite, suggesting an original reducing soil environment at these sampled depths. Mobile element concentrations relative to Ti (e.g. Ca/Ti, Na/Ti, Cs/Ti, Mg/Ti, Ni/Ti and Zn/Ti) show a marked depletion from the granite protolith to the paleosol, characteristic of leached weathering profiles, particularly in humid climates. K/Ti, Rb/Ti and A-CN-K plots of two samples show alkali element enrichment which may have occurred during K-metasomatism, but overall this is a minor geochemical feature which has not affected the other analyzed samples.

Chondrite normalized paleosol REE profiles show negative Ce and Eu anomalies. When normalized to the "basement" granite significant fractionation of paleosol REE is evident (Fig. 2C). Heavy (H) REE are several orders of magnitude enriched compared to light (L) REE; this may occur following intensive chemical weathering (Yusoff et al., 2013), especially when organic-rich topsoil exists (Nesbitt, 1977). Organic-rich soil waters at lowered pH are particularly aggressive in removing REE (Nesbitt & Marcovics, 1997). Estimates of Archean atmospheric CO_2 concentration are 10^1 PAL, which may have resulted in a rainwater pH of c. 4.6 (Ohmoto et al., 2004). Incipiently and moderately altered rocks are known to be particularly enriched in HREE in alteration zones from lower parts of soil profiles, while extremely altered residual products in upper parts are commonly depleted in HREE (Nesbitt, 1977; Yusoff et al., 2013; Berger et al., 2014). Preferential HREE enrichment in the preserved portion of the Keonjhar Paleosol profile, as well as lower Fe_T/Ti and Mn/Ti and higher V/Ti with respect to the granite protolith therefore indicate the preserved level of the paleosol most likely represents the lower part of the original soil profile and alteration zone. Significantly, all paleosol samples show true negative Ce anomalies, calculated as chondrite normalized Ce/Ce*-Pr/Pr* (Fig. 2C). The presence of a negative Ce-anomaly and HREE enrichment in the Keonjhar Paleosol suggest development of a zoned soil profile analogous to modern tropical "lateritic" profiles with distinct wet and dry seasons (Fitzpatrick, 1986). In lateritic soil profiles the upper part is oxidized where Mn and Fe oxy-hydroxides accumulate as a Fe-Mn duricrust (Duzgoren-Aydin & Aydin, 2009). The pallid zone immediately below the duricrust bears signatures of a reducing environment from which soluble Fe^{2+} and Mn^{2+} migrate and precipitate at the top oxidized part during dry seasons (Beukes et al., 2002). Negative Ce anomalies may form in regions of the soil profile where REE except Ce have accumulated from an overlying oxidized zone. This occurs when Ce^{3+} is transformed to the highly immobile Ce^{4+}, possibly involving cerianite ($Ce^{(IV)}$O2) precipitation, so that Ce retained in the upper soil profile and fractionated with respect to trivalent REE (Berger et al., 2014). In this way, Ce is preferentially retained with Mn and Fe oxy-hydroxides in a lateritic duricrust. The Keonjhar Paleosol now preserved below the sandstone likely represents the pallid alteration zone of the lower part of a "lateritic" soil profile marked by the characteristic Fe, Mn depletion, HREE enrichment and a negative Ce-anomaly.

It is highly significant that siliciclastic sediments unconformably overlying the paleosol do not demonstrate any mineralogical evidence for Fe-Mn enrichment. Furthermore, there is no silicification, albitization or enrichment of diagnostic elements (e.g. Zn, Cu, W, Sn, Mo) to support hydrothermal fluid passage along the granite-sandstone unconformity. The described mineralogical and geochemical features of the Keonjhar Paleosol therefore formed during a period of chemical weathering when the granite surface was exposed to the atmosphere and that this occurred prior to deposition of the overlying siliciclastic sequence.

CONCLUSIONS

The presence of both oxidative weathering in the Keonjhar Paleosol and the presence of redox sensitive minerals in the overlying quartzarenite may either signify a decrease in atmospheric oxygen between paleosol formation and deposition of the overlying siliciclastics, or alternatively that atmospheric oxygen was sustained at a relatively narrow concentration interval (between c. 10^{-4} and 10^{-3} PAL) capable of sustaining both these features. Formation of the Keonjhar Paleosol signifies the presence of molecular oxygen at levels above those which could have been produced by photo-dissociation of atmospheric water alone (Kasting and Walker, 1981). We propose this early, transient atmospheric oxygenation was due the existence of micro-organisms capable of oxygenic photosynthesis. This is dramatically earlier than most previous estimates for the development of photosynthesis (Des Marais, 2000; Farquhar et al., 2011), but is not inconsistent with its development as a metabolic process prior to the evolution of an entire genome for a photosynthetic organism (Xiong et al., 2000).

Previous attempts to compile chemical and isotopic data from Archean paleosols have been limited by the small number of definite paleosols known from early Earth history (Rye and Holland, 1998). Our study of the Keonjhar Paleosol highlights the importance of new discoveries of such horizons in constraining atmospheric evolution at a higher temporal resolution. These rare examples of paleosols from deep time provide the potential to link geological, biological and environmental evidence to build a more comprehensive understanding of secular changes in the early Earth System.

ACKNOWLEDGEMENTS

This work is supported by research funding from BRNS-India to JM and GG, a DST-India (SR/WOS-A/ES-10/2010) grant to SG and a Trinity College Dublin (TCD) FEMS project fund to QGC, JM and GG. Thanks to Balz Kamber for his generous support in providing additional analytical time at TCD for U-Pb zircon analyses. This work forms part of PhD research by of KC and BM. JM, GG and SB acknowledge FRPDF grant from

Presidency University and a CSIR Research grant. UGC-CAS and DST-FIST laboratory facilities at Presidency University have been used. JM, GG and QGC acknowledge logistic support provided by Tata Steel during fieldwork. JM dedicates his contribution in memory of his teacher the Late Professor Asru Kumar Chaudhuri.

REFERENCES CITED

Acharyya, S. K., Gupta, A., and Orihashi, Y., 2010, Neoarchean–Paleoproterozoic stratigraphy of the Dhanjori basin, Singhbhum Craton, Eastern India: And recording of a few U–Pb zircon dates from its basal part: Journal of Asian Earth Sciences, v. 39, p. 527-536.

Anbar, A.D., Duan, Y., Lyons, T.W., Arnold, G.L., Kendall, B., Creaser, R.A., Kaufman, A.J., Gordon, G.W., Scott, C., Garvin, J., and Buick, R., 2007, A whiff of oxygen before the great oxidation event?: Science, v. 317, p. 1903-1906.

Bandopadhyay, P.C., Eriksson, P.G., and Roberts, R.J., 2010, A vertic paleosol at the Archean-Proterozoic contact from the Singhbhum-Orissa craton, Eastern India: Precambrian Research, v. 177, p. 277-290.

Berger, A., Janots, E., Gnos, E., Frei, R., and Bernier, F., 2014, Rare earth element mineralogy and geochemistry in a laterite profile from Madagascar: Applied Geochemistry, v. 41, p. 218-228.

Bekker, A., Holland, H.D., Wang, P.L., Rumble, D., Stein, H.J., Hannah, J.L., Coetzee, L.L., and Beukes, N.J., 2004, Dating the rise of atmospheric oxygen: Nature, v. 427, p. 117–120.

Beukes N.J., Dorland, H., Gutzmer, J.G., Nedachi, M., and Ohmoto, H., 2002, Tropical laterites, life on land, and the history of atmospheric oxygen in the Paleoproterozoic: Geology, v. 30, p. 491–494.

Canfield, D.E., Habicht, K.S., and Thamdrup, B., 2000, The Archean sulfur cycle and the early history of atmospheric oxygen: Science, v. 288, p. 658–661.

Crowe, S.A., Døssing, L.N., Beukes, N.J. Bau, M., Kruger, S.J., Frei, R., and Canfield, D. E., 2013. Atmospheric oxygenation three billion years ago: Nature, v. 501, p. 535-539.

Des Marais, D.J., 2000, When did photosynthesis emerge on Earth?: Science, v. 289, p. 1703-1705.

Duzgoren-Aydin, N.S., and Aydin, A., 2009, Distribution of rare earth elements and oxyhydroxide phases within a weathered felsic igneous profile in Hong Kong: Journal of Asian Earth Sciences, 34, p. 1-9.

Farquhar, J., Bao, H., and Thiemens, M., 2000, Atmospheric influence of Earth's earliest sulfur cycle: Science, 289, p. 756-758.

Fitzpatrick, E.A., 1986, An introduction to soil science: Longman Scientific and Technical, Essex, 255 p.

Holland, H.D., 2006, The oxygenation of the atmosphere and oceans: Philosophical Transactions of the Royal Society of London, ser. B, v. 361, p. 903–915.

Johnson, I.J., Watanabe, Y., Yamaguchi, K., Hamasaki, H., and Ohmoto, H., 2008, Discovery of the oldest (~3.4 Ga) lateritic paleosols in the Pilbara Craton Western Australia: Geological Society of America Abstracts with Programs, v. 40, p. 143.

Kasting, J.F., and Walker, J.C.G., 1981, Limits on oxygen concentration in the prebiological atmosphere and the rate of abiotic fixation of nitrogen: Journal of Geophysical Research, v. 86, p. 1147-1158.

Kumar, A., Venkatesh, A.S., Ramesh Babu, P.V.R., and Nayak, S., 2012, Genetic implications of rare uraninite and pyrite in quartz-pebble conglomerates from Sundargarh District of Orissa, Eastern India: Journal of the Geological Society of India, v. 79, p. 279-286.

Langmuir, D. 1997, Aqueous environmental geochemistry. Prentice Hall, NJ, 600p.

Lyons, T.W., Reinhard, C.T., and Planavsky, N.J., 2014, The rise of oxygen in Earth's early ocean and atmosphere: Nature, v. 506, p. 307-315.

Macfarlane A.W., Danielson, A., and Holland, H.D., 1994, Geology and major and trace element chemistry of the late Archean weathering profiles in the Fortescue Group, Western Australia: Implications for atmospheric PO_2: Precambrian Research, v. 65, p. 297–317.

Misra, S., Moitra, S., Bhattacharya, S., and Sivaraman T.V., 2000, Archean Granitoids at the contact of Eastern Ghat granulite belt and Singhbhum-Orissa craton in Bhuban Rengali Sector, Orissa, India: Gondwana Research, v. 3, p. 205-213.

Mukhopadhyay, J., Beukes, N.J., Armstrong, R.A., Zimmermann, U., Ghosh, G., and Medda, R.A. 2008, Dating the Oldest Greenstone in India: A 3.51-Ga Precise U-Pb SHRIMP Zircon Age for Dacitic Lava of the Southern Iron Ore Group, Singhbhum craton: Journal of Geology, v. 116, p. 449-461.

Mukhopadhyay, J., Ghosh, G., Zimmermann, U., Guha, S., and Mukherjee, T., 2012, A 3.51 Ga bimodal volcanics-BIF-ultramafic succession from Singhbhum Craton: implications for Palaeoarchaean geodynamic processes from the oldest greenstone succession of the Indian subcontinent: Geological Journal, v. 47, p. 284–311.

Nesbitt, H. W., 1977, Mobility and fractionation of rare earth elements during weathering of a granodiorite: Nature, v. 279, p. 206-210.

Nesbitt, H.W., and Markovics, G., 1997, Weathering of granodioritic crust, long-term storage of elements in weathering profiles, and petrogenesis of siliciclastic sediments: Geochimica et Cosmochimica Acta, v. 61, p. 1653-1670.

Ohmoto H., Watanabe Y., and Kazumasa K., 2004, Evidence from massive siderite beds for a CO_2-rich atmosphere before ~1.8 billion years ago: Nature, v. 429, p. 395-399.

Ohmoto, H., 1996, Evidence in pre-2.2 Ga paleosols for the early evolution of atmospheric oxygen and terrestrial biota: Geology, v. 24, p. 1135-1138.

Philippot, P., Teitler, Y., Gérard, M., Cartigny, P., Muller, E., Assayag, N., Le Hir, G., and Fluteau, F. 2013, Isotopic and Mineralogical Evidence for Atmospheric Oxygenation in 2.76 Ga Old Paleosols: Mineralogical Magazine, v. 77, p. 1965.

Planavsky, N.J., Asael, D., Hofmann, A., Reinhard, C.T., Lalonde, S.V., Knudsen, A., Wang, X., Ossa Ossa, F., Pecoits, E., Smith, A.J.B., Beukes, N.J., Bekker, A., Johnson, T.M., Konhauser, K.O., Lyons, T.W., and Rouxel, O.J., 2014, Evidence for oxygenic photosynthesis half a billion years before the Great Oxidation Event: Nature Geoscience, 7, p. 283-286.

Rosing, M.T., and Frei, R., 2004, U-rich Archaean sea-floor sediments from Greenland - indications of > 3700 Ma oxygenic photosynthesis: Earth and Planetary Science Letters, v. 217, p. 237-244.

Rye, R., and Holland, H.D., 1998, Paleosols and the evolution of atmospheric oxygen: A critical review: American Journal of Science, v. 298, p. 621–672.

Tait, J., Zimmermann, U., Miyazaki, T., Presnyakov, S., Chang, Q., Mukhopadhyay, J., and Sergeev, S., 2011, Possible juvenile Palaeoarchaean TTG magmatism in eastern India and its constraints for the evolution of the Singhbhum craton: Geological Magazine, v. 148, p. 340 - 347.

Xiong, J., Fischer, W.M., Inoue, K., Nakahara, M., and Bauer, C.E. 2000, Molecular Evidence for the early evolution of photosynthesis: Science, v. 289, p. 1724-1730.

Yang, W., Holland, H.D., and Rye, R., 2002, Evidence for low or no oxygen in the late Archean atmosphere from the 2.76 Ga Mt. Roe #2 paleosol, Western Australia: Part 3: Geochimica et Cosmochimica Acta, v. 66, p. 3707-3718.

Yusoff, Z.M., Ngwenya, B.T., and Parsons, I., 2013, Mobility and fractionation of REEs during deep weathering of geochemically contrasting granites in a tropical setting, Malaysia: Chemical Geology, v. 349-350, p. 71-86.

GSA Data Repository item 2014xxx, [Tables DR1 & DR2, U-Pb Detrital zircon ages (LA-ICPMS at Trinity College Dublin), and major and trace element concentrations of samples from Keonjhar Paleosol profile (Analyses by ACME LAB, Canada)] are available online at www.geosociety.org/pubs/ft2014.htm, or on request from editing@geosociety.org or Documents Secretary, GSA, P.O. Box 9140, Boulder, CO 80301, USA. Major element analyses were carried out by ICP-OES, whereas trace element and REE concentrations and U-Pb isotope ratios were determined by solution mode and laser ablation ICP-MS respectively.

FIGURE CAPTIONS

Figure 1A. Simplified geological map of the southern part of the Singhbhum Craton showing distribution of siliciclastic sediments unconformably overlying the Keonjhar Paleosol, Singhbhum Granite & Iron Ore Group greenstone. 1B. Field photograph of the paleosol overlain by quartzarenite sandstone (hammer rests on uneven basal erosional surface). 1C. BSEM image of detrital uraninite from quartzarenite and EDS spectrum showing uranium (U), lead (Pb) and oxygen (O) peaks. 1D BSEM image showing detrital pyrite (p) and uraninite (u) in quartzarenite. 1E. SEM image of pyrophyllite in the paleosol.

Figure 2A. Probability-age plot of 431 detrital zircon analyses (<10% discordant) from seven quartzarenite sandstone samples overlying the Keonjhar Paleosol. The youngest zircon population, indicated with an arrow, occurs at 3.02 Ga. The timing of the Great Oxygenation Event (GOE) as well as ages for formation for the Mt. Roe, Nsuze and Pilbara paleosols are indicated. 2B. Geochemical plots of paleosol samples. For Ti-normalized plots of paleosol samples, note enrichment/depletion with respect to basement granite shown as circles at base of each plot. 1C. REE composition of the Keonjhar Paleosol. Note HREE enrichment and negative Ce-anomaly in the paleosol with respect to granite protolith. Comparison with Pr-anomaly rules out effects of La-enrichment.

Fig. 1

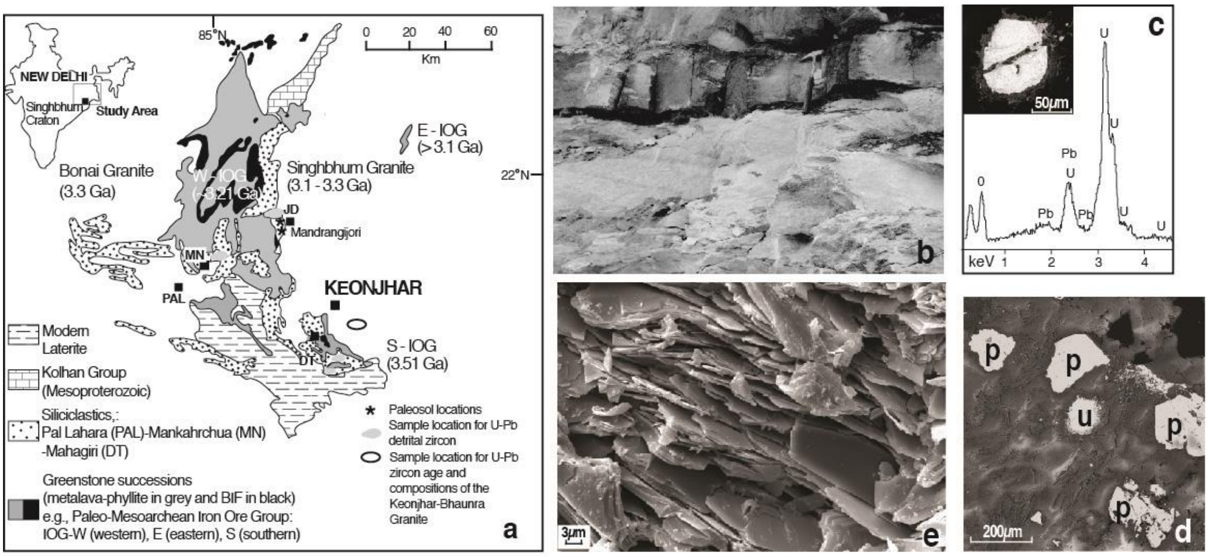

NEW DELHI
Singhbhum Craton
Study Area
Bonai Granite
(3.3 Ga)
W - IOG
Singhbhum Granite
(3.1 - 3.3 Ga)
E - IOG
(> 3.1 Ga)
JD
Mandrangjori
MN
PAL
KEONJHAR
DT
S - IOG
(3.51 Ga)
Km
Modern Laterite
Kolhan Group (Mesoproterozoic)
Siliciclastics,: Pal Lahara (PAL)-Mankahrchua (MN) -Mahagiri (DT)
Greenstone successions (metalava-phyllite in grey and BIF in black) e.g., Paleo-Mesoarchean Iron Ore Group: IOG-W (western), E (eastern), S (southern)
Paleosol locations
Sample location for U-Pb detrital zircon
Sample location for U-Pb zircon age and compositions of the Keonjhar-Bhaunra Granite
a
b
c
50μm
keV
d
200μm
e
3μm

Fig. 2

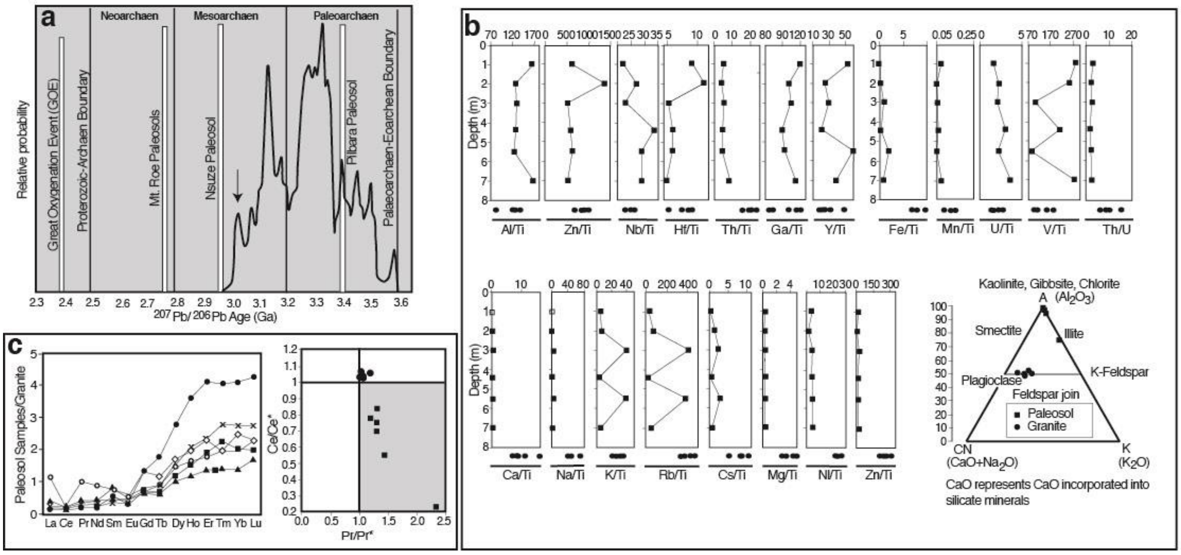

a
Neoarchaen
Mesoarchaen
Paleoarchaen
Relative probability
Great Oxygenation Event (GOE)
Proterozoic-Archaen Boundary
Mt. Roe Paleosols
Nsuze Paleosol
Pilbara Paleosol
Palaeoarchaen-Eoarchean Boundary
207Pb/206Pb Age (Ga)
b
Depth (m)
Al/Ti
Zn/Ti
Nb/Ti
Hf/Ti
Th/Ti
Ga/Ti
Y/Ti
Fe/Ti
Mn/Ti
U/Ti
V/Ti
Th/U
Ca/Ti
Na/Ti
K/Ti
Rb/Ti
Cs/Ti
Mg/Ti
Ni/Ti
Zn/Ti
Kaolinite, Gibbsite, Chlorite
A (Al2O3)
Smectite
Illite
K-Feldspar
Plagioclase
Feldspar join
Paleosol
Granite
CN (CaO+Na2O)
K (K2O)
CaO represents CaO incorporated into silicate minerals
c
Paleosol Samples/Granite
La Ce Pr Nd Sm Eu Gd Tb Dy Ho Er Tm Yb Lu
Ce/Ce*
Pr/Pr*

Table DR1.

LA-ICP-MS U-Pb detrital zircon data from quartzarenites from Mahagiri, Pal-Lahara-Mankaharchua Range and from north of Keonjhar. Percentage discordance calculated as a difference betweeen $^{207}Pb/^{206}Pb$ and $^{206}Pb/^{238}U$ ages. Analyses marked * are >10% discordant and are not used in construction of the probability diagram. 431 out of 770 analyses are <10% discordant.

Table DR2.

Major (wt%) and trace element (ppm) concentrations of samples from Keonjhar Paleosol profile.

Online Section

FULL METHODS

Major, trace and rare earth element analyses were carried out at the ACME Analytical Laboratories (Vancouver) Ltd. Major elements were determined using a SPECTRO ARCOS ICP-optical emission spectrometer (ICP-OES) following a lithium borate fusion and dilute acid digestion. Loss on ignition (LOI) was determined by sintering at 1000°C and Leco analysis was carried out for total carbon and sulphur. Trace element concentrations, including rare earth elements (REE), were carried out using a NexION 300 ICP-MS.

All sandstone samples for the U-Pb zircon aspect of the study were prepared and analysed at Trinity College Dublin, Ireland. Rocks were crushed, milled using a Retsch® DM-200 disc mill fitted with manganese steel grinding discs, sieved to 300μm with the finer grained fraction separated using a Gemini® mineral separation table, a Frantz® magnetic separator (to 1.0A) and finally a methelyene iodide heavy liquid separation. Following mineral separation zircon from each sample was pipetted in ethanol and mounted in an epoxy grain mount, ground down to expose grain interiors and polished using 6µm and 1µ diamond pastes. A Photon Machines Analyte Excite laser ablation system with a 30µm spot size was used for ablations using the following settings: 28% power, repetition rate of 4Hz and 180 shot counts. This equates to a fluence of 3.3 J cm^{-2} and an ablation pit depth of approximately 15µm. The laser ablation system was coupled to a Thermo Scientific iCAP® (model S) quadrupole ICP-MS for isotope ratio measurements. Ablated material was transported to the plasma using ultrahigh purity He which was passed through an inline Hg trap. High purity Ar was employed as the plasma gas. 91500 (Wiedenbeck et al., 2004) was used as the primary zircon standard to corrected for any laser or plasma induced fractionation. Both Temora (Black et al., 2003) and Plešovice (Sláma et al., 2008) zircon were used as secondary standards to assess accuracy and reproducibility. Typically two primary and two secondary standard analyses were conducted for every 10 to 15 unknowns. Raw data were processed using the VizualAge data reduction scheme (Petrus and Kamber, 2012) operating within Iolite (Paton et al., 2011). Secondary standard data from several separate analytical sessions give $^{206}Pb/^{238}U$ ages of 417.6±3.1 Ma (MSWD=5.6) for Temora-1 and 337.2±2.0 Ma (MSWD=8.0) for Plešovice, which are within error of accepted values of 416.75±0.24 Ma (Black et al., 2003) and 337.13±0.37 Ma (Sláma et al., 2008) respectively. All U-Pb analyses reported are non-common Pb corrected. A $^{206}Pb/^{238}U$ versus $^{207}Pb/^{206}Pb$ age discordance was calculated for all unknowns and only analyses less than 10% discordant were used in construction of probability-age diagrams using Isoplot (Ludwig, 2003).

Black, L. P. et al., 2003, TEMORA 1: A new zircon standard for Phanerozoic U-Pb geochronology: Chemical Geology, v. 200, p. 155–170.

Ludwig, K. R., 2003, Isoplot / Ex 3.00. A geochronological toolkit for Microsoft Excel: Special Publication 4, Berkeley Geochronological Center (Berkeley, CA, USA), 70 p.

Paton, C. et al., 2011, Iolite: Freeware for the visualization and processing of mass spectrometric data: Journal of Analytical Atomic Spectroscopy, v. 26, p. 2508–2518.

Petrus, J. A., and Kamber, B. S., 2012, VizualAge: A Novel Approach to Laser Ablation ICP-MS U-Pb Geochronology Data Reduction: Geostandards and Geoanalytical Research, v. 36, p. 247-270.

Sláma, J. et al., 2008, Plěsovice zircon – A new natural reference material for U-Pb and Hf isotopic microanalysis: Chemical Geology, v. 249, p. 1–35.

Wiedenbeck, M., et al., 2004, Further characterization of the 91500 zircon crystal: Geostandards and Geoanalytical Research, v. 28, p. 9–39.